Common Path Heterodyne Optical Fiber Sensors

Toshihiko Yoshino, Takaharu Hashimoto, Makoto Nara, and Kiyoshi Kurosawa

Abstract— **The common path type of differential heterodyne fiber-optic sensing scheme has been developed which uses a polarization maintaining fiber as either a sensor or an optical lead and a dual-frequency dual-polarization laser beam. The sensing schemes are applied to the measurements of temperature, strain, force, pressure, rotation rate (gyro), magnetic and electric fields, and thin film thickness. The sensing scheme and main performances for each measurand are described. High precision and high stability as well as good linearity for each measurand are demonstrated.**

I. Introduction

BY means of optical fiber sensors many physical and chemical quantities can be measured in a flexible and remote manner without undergoing electromagnetic induction noises. However, at the present stage of fiber-optic sensing technology, high stability and reliability are the most required features for practicing fiber sensors. In order to fulfill such requirements, the present authors have developed the common path type of heterodyne optical fiber sensing in which heterodyning two laser beams take a common path in the entire sensing system since 1981. The sensing system can measure various quantities with good linearity and high stability against environmental temperature and pressure variations.

The key devices for the developed fiber sensors are a dual-frequency dual-polarization laser beam and a polarization-maintaining fiber, which are used for a sensor element or an optical lead. The combination of the two devices produces a stable and precise fiber sensing scheme especially suited for polarization based fiber sensors. The developed fiber sensors make it possible to measure various quantities such as temperature, strain, force, pressure, rotation rate (gyroscope), magnetic and electric fields, displacement, and film thickness. The purpose of this paper is to give the detailed descriptions of our previous studies on the in-line heterodyne fiber sensors, partially reported in the several conferences [1]–[7]. The sensing schemes and main performances of the developed fiber sensors are described classifying the use of polarization maintaining fiber (PMF) into a sensor element and an optical lead.

Manuscript received October 31, 1990. This work was partially supported by Grant-in-Aid for Special Project Research for Lightwave Sensing from the Ministry of Education, Science, and Culture of Japan.

T. Yoshino is with the Department of Electronic Engineering, Faculty of Engineering, Gunma University, Tenjincho, 1-5-1, Kiryu, Gunma, Japan.

T. Hashimoto is with Tokyo Sokki Kenkyujo Co., Ltd., Aioicho, 4-247, Kiryu, Gunma, Japan.

M. Nara is with Nikon, Nagaodai-machi 4-7-1, Totsuka-ku, Yokohama, Japan.

K. Kurosawa is with the Tokyo Electric Power Inc., Nishi-tutujigaoka 2-4-1, Chohu, Tokyo, Japan.

IEEE Log Number 9106098.

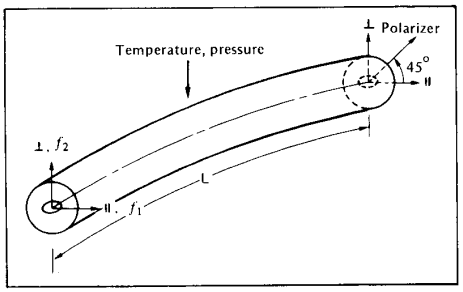

Fig. 1. Optical arrangement of heterodyne fiber-optic sensor using polarization maintaining fiber as sensor element.

II. Use of PMF as Sensor Element

The retardation of highly birefringent single-mode fiber, i.e., polarization maintaining fiber (PMF), depends on temperature and mechanical forces so that it can be used for temperature (e.g., [8]) or mechanical force measurement. Here we present a new sensing scheme to achieve high precision for the retardation measurement.

A laser beam consisting of two frequency components with orthogonal linear polarization is launched into a PMF with the coincidence of polarization axes between the laser and PMF, as shown in Fig. 1. The output beam from PMF is passed through a polarizer oriented at 45° to the fiber polarization axes, ∥ and ⊥, and detected by a photomultiplier. Letting the propagation constants of the orthogonal polarization modes of the fiber be $\beta_{\parallel}$ and $\beta_{\perp}$ and the laser frequencies be f_1 and f_2, the photoelectric signal is given by

$$I = |A_{\parallel} \exp i(2\pi f_1 t - \beta_{\parallel} L) + A_{\parallel} \exp i(2\pi f_2 t - B_{\perp} L)|^2 \tag{1}$$

where L is the fiber length and $A_{\parallel}$ and $A_{\perp}$ are real constants. Equation (1) represents a beat signal

$$I = A_{\parallel}^2 + A_{\perp}^2 + 2A_{\parallel}A_{\perp}\cos\{2\pi(f_1 - f_2)t - (\beta_{\parallel} - \beta_{\perp})L\} \tag{2}$$

which can be rewritten as

$$I = A + B\cos(2\pi\Delta f t - \Gamma), \quad (\Delta f = f_1 - f_2;\ A, B \text{ real numbers}) \tag{3}$$

where

$$\Gamma = (\beta_{\parallel} - \beta_{\perp})L \tag{4}$$

is the retardation of PMF, depending on temperature and applied force besides the initial retardation.

The PMF used in this paper is Hitachi Cable's one having a beat length of 2.5 mm at 20°C and $\lambda = 633$ nm.

The light source used is a home-made frequency stabilized transverse Zeeman He–Ne laser operated at $\lambda = 633$ nm (STZL). The laser emits orthogonally linearly polarized two modes having a frequency separation from 300 to 400 kHz, stabilized within about 1 kHz; the frequency stabilization was achieved by the negative feedback of the beat frequency of the two modes to the cavity length by means of a cooling fan [9].

A. Temperature

Fig. 2(a) shows the temperature sensing system. In order to locate the sensing part at a specified section of the fiber and to eliminate the effect of the surrounding temperature variations, a differential detection scheme using two PMF's is employed. Both a signal fiber and a reference fiber are aligned close to each other except the sensing part, where the sensing fiber was made longer than the reference one by different lengths L of 0–4 m; the entire length of the sensing fiber was 10 m. The sensing part was inserted in a water bath, heated by a nichrome heater inserted in the water. Fig. 2(b) shows the typical beat signals (300 kHz) of the sensing and reference fibers. The phase difference between the two beat signals is detected by a phasemeter. Fig. 2(c) shows the change in phasemeter output measured as a function of the change in water temperature monitored with a mercury thermometer. In the experiment the water bath was heated and natural-cooled many times. Somewhat data variations observed in Fig. 2(c) are most probably due to the temperature inhomogeneity within the bath. The temperature dependence of fiber retardation is given, from the average slope of Fig. 2(c), as

$$d\Gamma/LdT = 114^\circ\,^\circ\mathrm{C}^{-1}\mathrm{m}^{-1}. \tag{5}$$

The temperature resolution ΔT is proportional to the sensing fiber length L and limited by the fluctuation of the phasemeter output, $\Delta\Gamma$, which was about 0.1°. From (5), ΔT is $0.1^\circ/(114^\circ\mathrm{C}^{-1}\mathrm{m}^{-1}L) = 0.009^\circ\mathrm{Cm}/L$, or 0.009°C for $L = 1$ m for example.

Thermal cycling was studied between room temperature and 185°C by inserting a 1-m-long part of PMF into an electric furnace. Fig. 2(d) shows the measured results in which temperature was raised from 30 to 185°C in one hour and fell down in natural cooling. A good reproducibility is shown in Fig. 2(d).

B. Strain and Force Sensors

Fig. 3(a) shows the strain sensing system. In order to reduce the temperature-induced drift, a differential detection scheme using two PMF's is again employed. A 27-mm-long part of a sensing PMF is fixed on an aluminium plate by a scotch tape whereas a reference PMF is aligned close to the sensing one but free from the plate. Axial strain was applied to the fiber by bending the plate and monitored by a metal strain gauge. Fig. 3(b) shows the change in the phasemeter output measured as a function of the monitored strain ε. The strain-induced retardation is proportional to the sensor length L and,

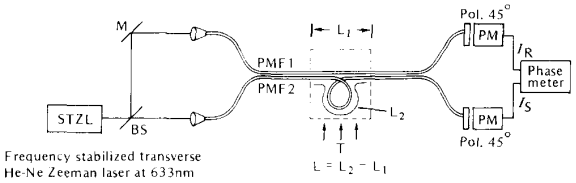

(a)

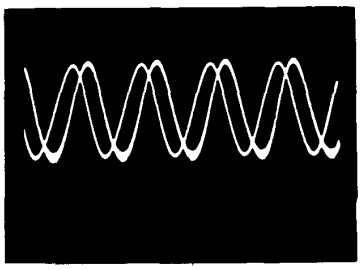

(b)

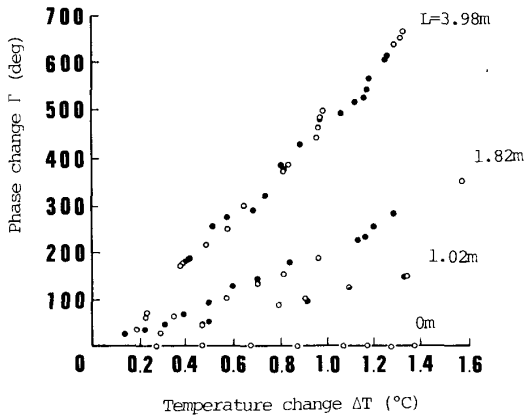

(c)

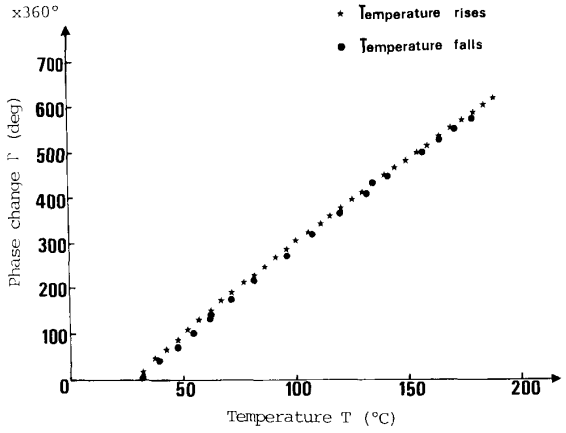

(d)

Fig. 2. Heterodyne fiber-optic temperature sensor using polarization maintaining fiber. (a) Measuring system. (b) Beat signals (signal and reference lights; the beat frequency = 300 kHz). (c) Temperature dependence of phasemeter output measured as a parameter of sensor fiber length L. (d) Thermal cycling of 1-m-long polarization maintaining fiber temperature sensor.

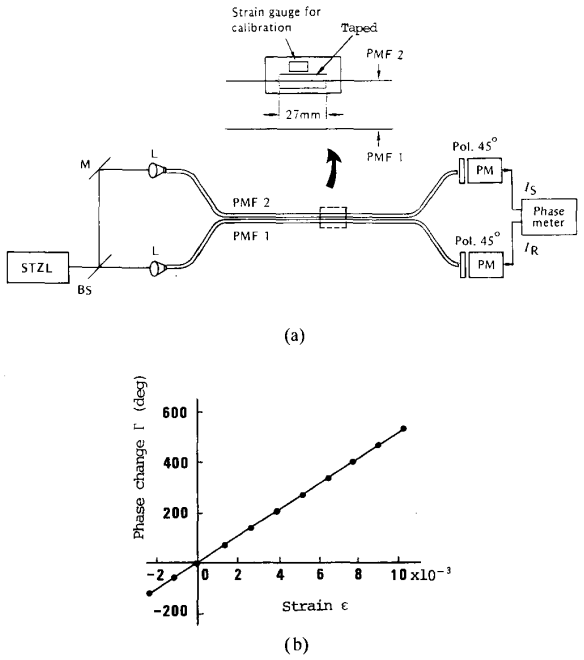

Fig. 3. Heterodyne fiber-optic strain sensor using polarization maintaining fiber. (a) Measuring system. (b) Phasemeter output measured as a function of applied strain.

from Fig. 3(b), is given as

$$d\Gamma/Ld\varepsilon = 500°/(27\text{ mm} \times 10 \times 10^{-3}\varepsilon) = 1.9 \times 10^{6°}\varepsilon^{-1}\text{m}^{-1}. \quad (6)$$

The minimum detectable strain is proportional to the sensor length. As the fluctuation of the phasemeter output was about 0.1°, the strain resolution $\Delta\varepsilon$ is, from (6), $0.1°/(1.9 \times 10^{6°}\varepsilon^{-1}\text{m}^{-1}L) = 5.3 \times 10^{-8}\varepsilon\text{m}/L$, or $0.053 \times 10^{-6}\varepsilon$ for $L = 1$ m for example.

In order to see the temperature compensation effect using two PMF's, the two fibers were inserted in an empire tube and heated over a 1-m-long part by a hair dryer. When the tube temperature was raised by 15°C, the change in the phasemeter output was 100° at worst in contrast with 2500° in the case of a single fiber. The temperature compensation effect is thus better than 1 : 25.

Various types of strain and force sensors can be constructed. Fig. 4(a) shows the measured result for a tension type of force sensor. An 170-mm-long part of PMF was cementized in a glass tube and axial tensile force was applied to the fiber by various weights. The force-induced retardation is proportional to the sensor length L and, from Fig. 4(a), is

$$d\Gamma/LdF = 600°/(0.2\text{ kgf} \times 170\text{ mm}) = 1.8 \times 10^{4°}\text{ kgf}^{-1}\text{m}^{-1}. \quad (7)$$

From (7), using $\Delta\Gamma = 0.1°$ the minimum detectable force ΔF is $0.1°/(1.8 \times 10^{4°}\text{ kgf}^{-1}\text{m}^{-1}L) = 5.6 \times 10^{-6}$ kgfm$/L$, or 0.0056 grf for $L = 1$ m for example.

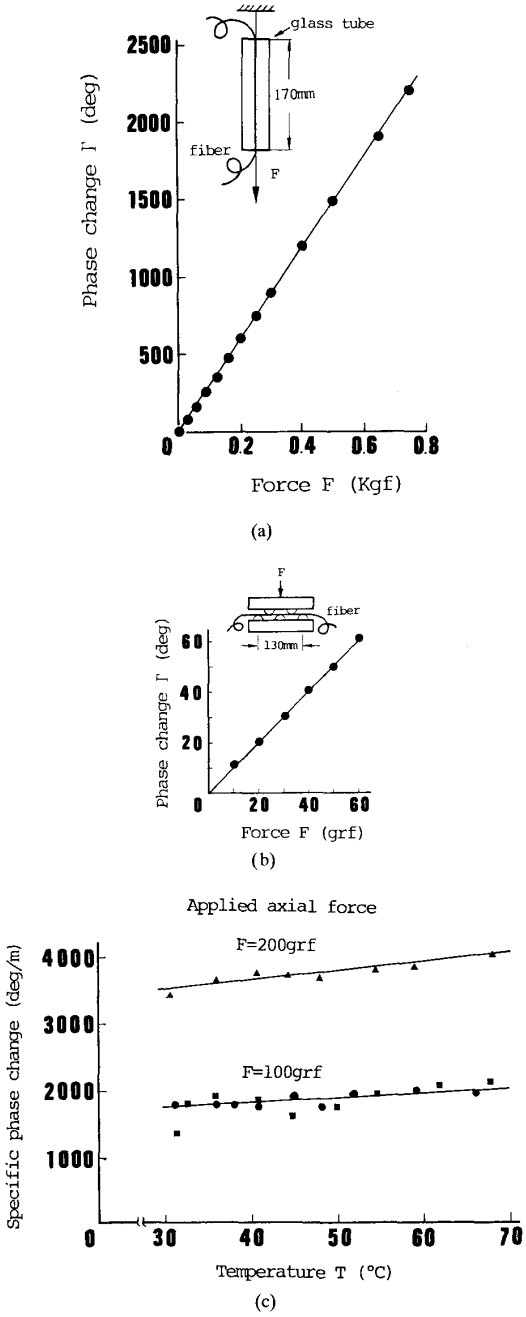

Fig. 4. Heterodyne fiber-optic force sensors using polarization maintaining fiber. (a) Tension type. (b) Microbending type. (c) Temperature dependence of force sensitivity.

Fib. 4(b) shows another type of force sensor using a microbender. An 130-mm-long part of PMF was sandwiched by two wave-form plates having a pitch of 20 mm. Various weights were loaded on the upper plate, causing dominantly axial tensile stress in the fiber. The minimum detectable force was about 1 grf.

The force-induced retardation was found to depend a little on fiber temperature. Fig. 4(c) shows the measured depen-

dence of force-induced retardation on temperature. The force-induced retardation increased with temperature. It follows from Fig. 4(c) that the force sensitivity of PMF increases with temperature in about 0.25%/°C.

C. Fiber Gyro

Fiber gyro is a rotation sensor using the Sagnac effect in the monomode fiber loop. Much work has been done to improve on the gyro performances [10]. Among them, an absolutely constant scale factor for rotation rate detection is one of the most desirable features for practical fiber gyros. Here we present a new type of fiber gyro fulfilling the requirement. The method is based on heterodyne detection, but, unlike the usual heterodyne method [11], the interfering two laser beams take a common path in the entire sensor system so that the gyro system becomes substantially stable against the environmental variations.

Fig. 5(a) shows the entire gyro system. The Sagnac ring interferometer consists of a polarization beam splitter PBS, two Faraday rotators FR1 and FR2, each producing $-45°$ and $+45°$ rotations of polarization plane, and a PMF coil. The orthogonally linearly polarized different frequency f_1 and f_2 components from a STZL are split by PBS into the CW and CCW traveling beams in the ring interferometer. The two beams undergo $\pm 45°$ rotations of polarization plane so that they can travel the PMF along a common polarization axis. The combination of one Faraday rotator and PBS makes an optical isolator so that both the CW and CCW beams going out of the ring interferometer don't return the laser source but go to a photomultiplier PM1.

The optical beat I_s generated at PM1 has a phase

$$\Phi = 2\pi \Delta f L/c + \phi_s \tag{8}$$

where $\Delta f = f_1 - f_2$, L is the total light path length from the light source to the photodetector, c is the light velocity in vacuum, and

$$\phi_s = (4\pi L_f a/\lambda c)\Omega \tag{9}$$

is the Sagnac shift [12], where a is the radius of the fiber coil, L_f is the fiber coil length, λ is the light wavelength in vacuum, and Ω is the rotation rate of the fiber coil. In the present experimental conditions, $a = 15$ cm, $L \approx L_f = 100$ m, and $\lambda = 633$ nm so that $\phi_s[\text{deg}] = 1.0\Omega[\text{deg/s}]$. The optical phase of the beat signal I_S was compared with that of the reference beat signal I_R taken from the back side of the laser. Somewhat phase fluctuations were observed in the phasemeter output but they could be reduced down to 0.1° by vibrating a short part of the fiber coil by means of a PZT driven at about 10 kHz. Three pictures of Fig. 5(b) shows the signal and reference beat signals observed when the fiber coil was at rest and rotated at $\Omega = \pm 38°/\text{s}$, respectively; the initial phase bias involved in the phasemeter output was removed; Fig. 5(c) shows the analog output signal of the phasemeter when the fiber coil was rotated by hand; the time constant of the phasemeter was 0.4 s. The minimum detectable rotation rate was then 0.1°/s. The phasemeter output involves a nonreciprocal phase bias due to the first term of (8), which depends on the amount of the beat frequency Δf and hence can vary with the beat frequency fluctuation. The associated phase fluctuations, however, can

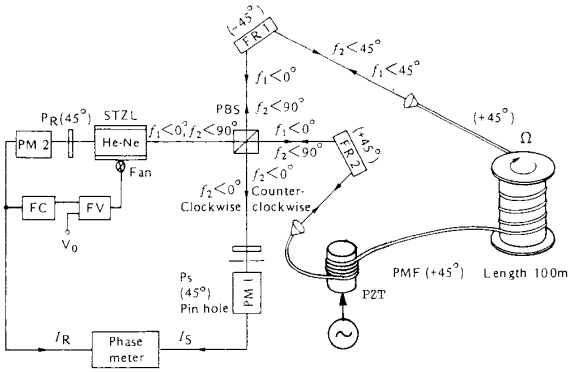

(a)

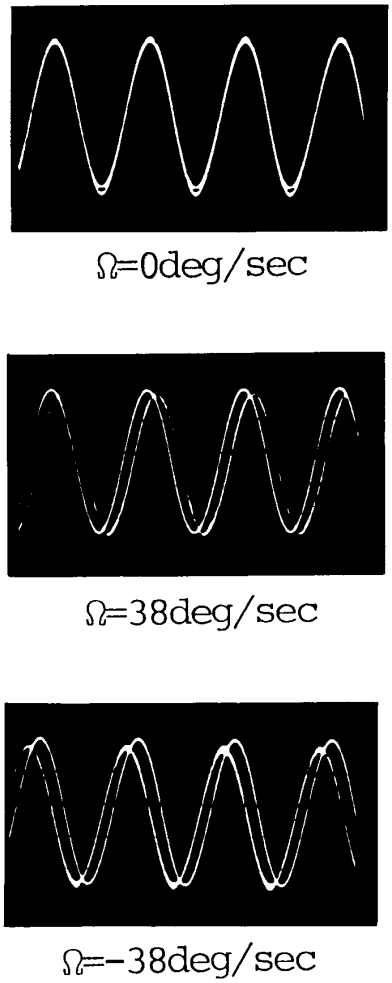

(b)

Fig. 5. Heterodyne fiber gyroscope. (a) Optical system. (b) Signal and reference optical beats (300 kHz) for different rotation rates of Ω. (c) Phasemeter output when the fiber coil was rotated by hand; the time constant of the phasemeter is 0.4 s.

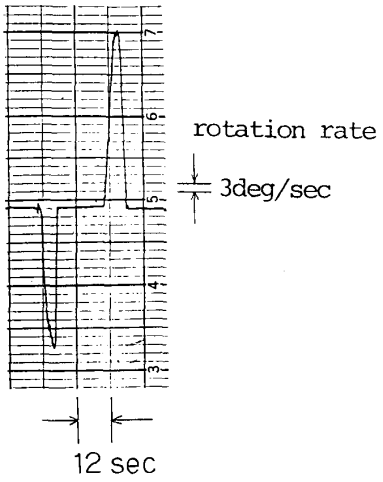

(c)

Fig. 5. (Continued)

be eliminated by passing the reference light through a fiber having a length equal to L.

III. Use of PMF as Optical Lead

There have been developed lots of types of fiber sensors which use optical fibers as optical leads to connect between optical transducers and light sources or photodetectors in order to realize flexible, *in-situ,* remote measurements. Among many types of such sensors, a polarimetric method is one of the most useful principles. The Faraday effect is used for the measurement of magnetic field [13], [14], the Pockels effect for voltage [14], the photoelastic effect for pressure [15], the natural birefringence for temperature [16] and the oblique light incidence for refractive index or film thickness [17]. In the previous polarization-based fiber sensors, however, optical fiber leads are mostly used to carry the intensity-modulated light signal, therefore being sensitive to light intensity fluctuations associated with fiber transmission, fiber coupling, light source fluctuations and so on. In this paper, intensity-insensitive fiber sensors are developed by the use of PMF as optical leads.

Fig. 6 shows the entire sensing setup for measuring various quantities such as magnetic field, voltage, pressure and temperature. The detection principle is based on the differential heterodyne scheme. The laser beam from a STZL is launched into a PMF (typically 10 m-long) with the mutual coincidence of polarization axes. Some part of the fiber was vibrated at about 5 kHz to reduce the fluctuation of the phasemeter output. The output light from the PMF is collimated by a SELFOC rod lens SL and incident on a polarimetric sensor cell. The laser beam emerging from the cell is, after passing through a polarizer oriented at 45° to the polarization axes of the sensor cell, sent to a photodetector through a fiber bundle. On the other hand, a light beam partially reflected from the entrance of the cell is detected and used for a reference light. Both the signal and reference lights generate the following beat

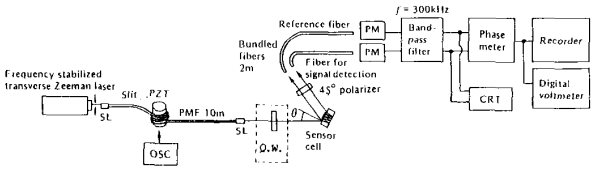

Fig. 6. Schematic diagram for fiber-optic differential heterodyne sensors using polarimetric sensor cell. PMF: polarization maintaining fiber, SL: self-focusing rod lens.

signals:

$$I_S = A_S \cos(2\pi\Delta f - \Phi - \Gamma) \tag{10a}$$

$$I_R = A_R \cos(2\pi\Delta f - \Gamma) \tag{10b}$$

where Φ is the retardation of the sensor cell, Γ is the retardation of PMF, and A_S and A_R are real numbers. The phase difference between the two beat signals is detected by a phasemeter. The minimum detectable retardation $\Delta\Gamma$ was about 0.1°.

A. Magnetic Field

In the measurement system of Fig. 6, the output light from PMF was passed through a quarter-wave plate QW to convert the incident light to the left and right circularly polarized lights. The sensor cell is made of FR5 glass, which has a Verdet constant V of -0.24 min cm^{-1} G^{-1} at $\lambda = 633$ nm. In order to enhance the measurement sensitivity, the multiple reflections of the light beam within a Faraday cell [18] were employed. The upper and lower surfaces of a 3.1-mm-thick 15 mm × 20 mm wide FR5 glass plate were coated with the multilayers of dielectric thin films having $\lambda/4$ optical thicknesses for oblique incidence so that the light beam may perfectly reflect with polarization maintaining. The light beam travels a zigzag path over a lateral region of 12.8 mm in the cell. Under the application of magnetic field, the cell material becomes circularly birefringent, thereby inducing phase retardation between the orthogonal circular polarizations, given by

$$\Phi_H = 2 \cdot 2N \cdot VHd \tag{11}$$

where H is the parallel component of magnetic field to the direction of cell thickness and $2N$ is the number of the multiple passes of light beam within the cell. Fig. 7(a) shows a typical pen recorder chart of the phasemeter output when H was ±50 Oe; the time constant of the phasemeter was 0.4 s. A very stable and precise measurement of dc magnetic field is achieved, which is very difficult by the conventional intensity modulation Faraday sensor. The minimum detectable dc field is less than 1 Oe. Fig. 7(b) and (c) respectively shows the phase changes measured as a function of relatively small and large dc magnetic fields. The cases of $2N = 40$ and 80 correspond to the angles of incidence on the cell surface 10° and 5°, respectively. The measured results of Fig. 7(a) and (b) agrees quite well with the theoretical ones, which, e.g., for $2N = 40$, $\Phi_H[\text{deg}] = 0.099H[\text{Oe}]$ calculated from (11). The present sensors can be used for ac fields too if the response

DOCKET ALARM

Explore Litigation Insights

Docket Alarm provides insights to develop a more informed litigation strategy and the peace of mind of knowing you're on top of things.

Real-Time Litigation Alerts

Keep your litigation team up-to-date with **real-time alerts** and advanced team management tools built for the enterprise, all while greatly reducing PACER spend.

Our comprehensive service means we can handle Federal, State, and Administrative courts across the country.

Advanced Docket Research

With over 230 million records, Docket Alarm's cloud-native docket research platform finds what other services can't. Coverage includes Federal, State, plus PTAB, TTAB, ITC and NLRB decisions, all in one place.

Identify arguments that have been successful in the past with full text, pinpoint searching. Link to case law cited within any court document via Fastcase.

Analytics At Your Fingertips

Learn what happened the last time a particular judge, opposing counsel or company faced cases similar to yours.

Advanced out-of-the-box PTAB and TTAB analytics are always at your fingertips.

API

Docket Alarm offers a powerful API (application programming interface) to developers that want to integrate case filings into their apps.

LAW FIRMS
Build custom dashboards for your attorneys and clients with live data direct from the court.

Automate many repetitive legal tasks like conflict checks, document management, and marketing.

FINANCIAL INSTITUTIONS
Litigation and bankruptcy checks for companies and debtors.

E-DISCOVERY AND LEGAL VENDORS
Sync your system to PACER to automate legal marketing.